PERGAMON

International Journal of Solids and Structures 38 (2001) 4685–4699

INTERNATIONAL JOURNAL OF SOLIDS and STRUCTURES

www.elsevier.com/locate/ijsolstr

An approximate algorithmic solution for the elastic fields in bonded patched sheets

C.N. Duong *, J.J. Wang, J. Yu

The Boeing Company, 2401 E. Wardlow Road, Mail Code C078-0209, Long Beach, CA 90807-5309, USA

Received 14 February 2000; in revised form 26 June 2000

Abstract

An approximate algorithmic solution is derived for the elastic fields in an infinite isotropic sheet rigidly bonded with an orthotropic, polygon-shaped patch. The approach employed here combines the equivalent inclusion method by Eshelby, see work by Mura (Micromechanics of Defects in Solids, 1987) and the extension of Rodin's (J. Mech. Phys. Solids 44, 1996) algorithmic solution for a polygonal inclusion with constant eigenstrains to the case of polynomial eigenstrains. A numerical example of an octagonal shaped patch symmetric with respect to two coordinate axes is presented using zero- and second-ordered approximation for eigenstrains, and the results are compared with those from finite element method. The study was motivated by the lack of analytical capabilities for analyzing and designing bonded repairs with a general shaped patch in aging aircraft.

Keywords: Composite bonded repair; Polygon-shaped inclusion; High ordered eigenstrain

1. Introduction

When today's aircrafts reach the end of their service lives, fatigue cracks are found to have developed along rivet holes and other highly stressed region of the aircraft. In order to extend the life of these aircraft, repairs have been made to arrest these cracks. The development of high-strength fibers and adhesives has made it possible to use composite bonded repairs for these situations. This repair scheme has shown to be very effective in arresting a crack and also eliminates stress concentrations at rivet holes created by mechanically fastened repairs.

Analytical method for analyzing crack patching using the inclusion analogy was first proposed by Rose (1981) for an elliptical patch. Rose's fundamental idea is to divide the analysis into two stages. The value of dividing the analysis into two stages is that different simplifying assumptions are appropriate for each stage. In stage I, the redistribution of stress in an *uncracked* skin due to the presence of the patch is determined, assuming that the skin and the patch are rigidly bonded. This assumption is appropriate in practice because the length of the load transfer zone around the edge of the patch is usually small

* Corresponding author. Tel.: +1-562-592-1421; fax: +1-562-982-7367.
E-mail address: cong.n.duong@boeing.com (C.N. Duong).

0020-7683/01/$ - see front matter
PII: S0020-7683(00)00296-1

compared with the overall dimension of the patch. Stage I problem is commonly referred to as a load attraction problem. For stage II, a problem of an infinite sandwiched plate consisting of a centered-cracked plate *adhesively* bonded to an uncracked reinforcing plate is considered. This two-stage analytical procedure provides a practical method to estimate quantities of primary interests such as the stress concentration factors near the edge of the patch and the crack tip stress intensity factor. However, stage I analysis had been carried out only for certain simple shapes such as ellipses or circles. The purpose of the present paper is to derive an approximate algorithmic close-form solution for the load attraction problem with a general shaped patch.

The terminology "inclusion", which will be mentioned throughout this paper, may have been used in a slightly different context in other papers on the bonded repair subject so that perhaps it needs a clarification. When a finite subdomain Ω in a homogeneous material D is prescribed by an initial strain (or eigenstrain) field and this initial strain field is zero outside Ω, then Ω is called an inclusion. If a subdomain Ω in a material D has elastic moduli different from those outside Ω, then Ω is called an inhomogeneity. The patching problem under present consideration is therefore classified as an inhomogeneity problem. The solution of the load attraction problem in a bonded (patched) sheet is solved by the Eshelby equivalent inclusion method combining with the algorithmic approach proposed recently by Rodin (1996) in his analysis of a polygonal and polyhedral inclusion under uniform eigenstrain. This approach is preferred over other methods such as Muskhelishvili complex variable method since literature contains numerous solutions for inclusion problems under uniform eigenstrain and these solutions can be extended to a case of polynomial eigenstrain in a straight forward manner. In contrast, the latter method requires a complex mapping for a non-elliptical patch and also an integration of a strain field resulting in multi-value functions.

As mentioned earlier, the elastic fields due to inclusions in an infinitely extended media have been investigated by many authors following the pioneering work of Eshelby (1957). Since a list of references on this subject is extensive and it can be found in Mura (1987), we will not discuss here all of those works. Only references most relevant to the present work will be cited. Elastic fields in a polygon-shaped inclusion with uniform eigenstrains in an infinitely extended isotropic media have been examined recently by Rodin (1996) and Nozaki and Taya (1997). However, no work has been done to extend these approaches to a case of polynomial eigenstrain and to apply them to the load attraction problem in a rigidly bonded sheet. On the other hand, elastic fields due to an ellipsoidal inclusion with eigenstrain given in the form of polynomials of coordinates have been obtained by Sendeckyj (1967) and Moschovidis (1975). Using these results, Moschovidis (Moschovidis, 1975; Moschovidis and Mura, 1975) employed the equivalent inclusion method to formulate the solution for a number of ellipsoidal inhomogeneities in an infinitely extended isotropic material. Johnson et al. (1980a,b) used the same approach to study the stress field in cuboidal precipitates. A similar approach will be taken here, but for a general shaped inhomogeneity. It should be emphasized that only an approximate solution is obtained for the current bonded problem since the condition for equivalency, as shown later in Section 2, can only be satisfied approximately using the first few terms of Taylor's series.

2. Equivalent inclusion method

In the equivalent inclusion method, the stress and strain fields induced by an inhomogeneity occupied region Ω will be the same as those induced by the strain field ε^*_{ij} in the same region of a homogeneous material C^0_{ijkl} when ε^*_{ij} is selected appropriately as shown in Fig. 1. The second problem in Fig. 1 is an inclusion problem. The equivalency condition between the two problems requires that

$$\varepsilon^{\mathrm{I}}_{ij} = \varepsilon^{\mathrm{II}}_{ij}, \qquad \sigma^{\mathrm{I}}_{ij} = \sigma^{\mathrm{II}}_{ij}, \tag{1}$$

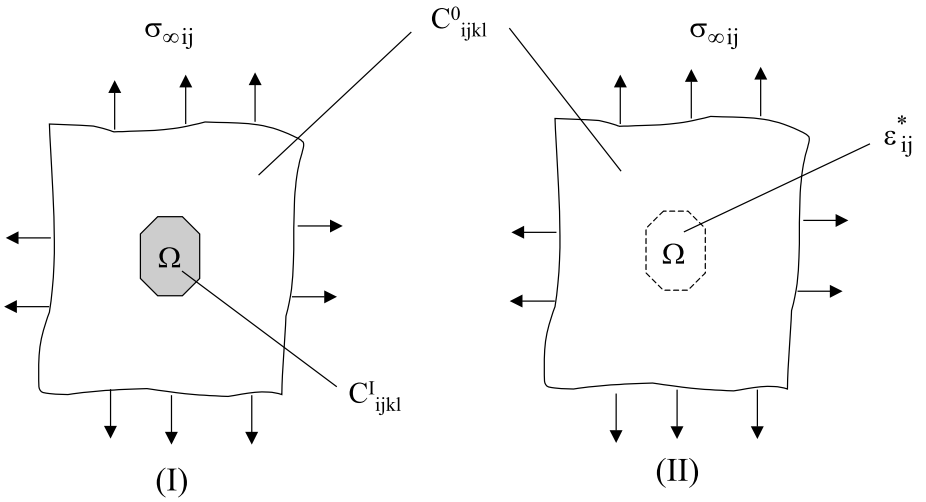

Fig. 1. An illustration of the equivalent inclusion method. (I) An inhomogeneity problem and (II) an inclusion problem with eigenstrains ε^*_{ij}.

at every point in subregion Ω. Since the second problem is an inclusion problem, the induced strain field in that problem is commonly expressed in terms of ε^*_{ij} and the far field applied strain $\varepsilon_{\infty ij}$ as (Mura, 1987)

$$\varepsilon^{\mathrm{II}}_{ij} = S_{ijkl}\varepsilon^*_{kl} + \varepsilon_{\infty ij}, \tag{2}$$

where S_{ijkl} is called Eshelby tensor. The next two sections will be devoted to the calculation of this Eshelby tensor for a polygon-shaped domain Ω with eigenstrains given in the form of polynomials of position coordinates. Similar to the thermal or initial strain, the resulting stress inside Ω for the second problem from Hook's law is

$$\sigma^{\mathrm{II}}_{ij} = C^0_{ijkl}\left(\varepsilon^{\mathrm{II}}_{kl} - \varepsilon^*_{kl}\right), \tag{3}$$

while the corresponding stress for the first problem equals

$$\sigma^{\mathrm{I}}_{ij} = C^{\mathrm{I}}_{ijkl}\varepsilon^{\mathrm{I}}_{kl}, \tag{4}$$

where C^{I}_{ijkl} is the elastic moduli of the inhomogeneity, C^0_{ijkl} is the elastic moduli of the material outside subregion Ω in problem I and also that of the homogeneous material in the second problem.

Substituting these results into Eq. (1) yields the following equation for ε^*_{ij}:

$$\begin{aligned} &\Delta C_{ijkl}S_{klmn}\varepsilon^*_{mn} - C^0_{ijkl}\varepsilon^*_{kl} = -\Delta C_{ijkl}\varepsilon_{\infty kl}, \\ &\Delta C_{ijkl} = C^0_{ijkl} - C^{\mathrm{I}}_{ijkl}. \end{aligned} \tag{5}$$

It should be noted that the above equation is non-linear because S_{ijkl} is an implicit function of ε^*_{ij}.

Eq. (5) will be solved approximately by the following procedure (Moschovidis, 1975; Moschovidis and Mura, 1975). First, ε^*_{ij} is assumed to be the polynomials of the position coordinates with yet to be determined coefficients, i.e.,

$$\varepsilon^*_{ij} = B_{ij} + B_{ijk}x_k + B_{ijkl}x_kx_l + \cdots \tag{6}$$

In Eq. (6), B_{ij}, B_{ijk}, B_{ijkl}, ..., are constants symmetric with respect to the free indices i, j and having value independent of the order in which the summation indices appear; i.e., $B_{ijkl} = B_{jikl}$, $B_{ijkl} = B_{ijlk}$. The Eshelby

tensors for an inclusion Ω with an eigenstrain equal to each term of the polynomials given in Eq. (6) are computed using Rodin's algorithmic approach for a polygonal inclusion. The details of these computations will be given in Sections 3 and 4, and let us assume for now that these Eshelby tensors are already obtained and denoted by $D_{ijkl}(\boldsymbol{x})$, $D_{ijklm}(\boldsymbol{x})$, and $D_{ijklmn}(\boldsymbol{x})$ for a constant, linear and quadratic eigenstrain, respectively. It should be noted that these tensors in general are not constant tensors, even for the case with uniform eigenstrains. Thus, from Eqs. (1) and (2)

$$\varepsilon_{ij}^{\mathrm{I}} = \varepsilon_{ij}^{\mathrm{II}} = \varepsilon_{\infty ij} + D_{ijkl}B_{kl} + D_{ijklm}B_{klm} + D_{ijklmn}B_{klmn} + \cdots \tag{7}$$

The next two steps are to expand these tensors D into Taylor series and to substitute these results into Eq. (5) together with Eq. (6). By setting the coefficient of each polynomial term of the resulting equation to zero, one obtains a system of algebraic equations with unknowns B_{ij}, B_{ijk}, and B_{ijkl}.

To illustrate the above procedure, we will formulate the solution for a polygon-shaped inhomogeneity that is symmetric with respect to two coordinate axes, in an infinitely extended isotropic media with uniform applied normal strains at infinity. In addition, the elastic moduli of the inhomogeneity are orthotropic with the material principal directions parallel to the coordinate axes. The double symmetry condition of the problem imposes that the normal component of the eigenstrains must be an even function of the coordinates while the shear component is an odd function. If the eigenstrain ε_{ij}^{*} is approximated by a second degree polynomial, then ε_{ij}^{*}, after taking into consideration the double symmetry condition, must presume the following form:

$$\begin{aligned}
\varepsilon_{11}^{*} &= B_{11} + x_1^2 B_{1111} + x_2^2 B_{1122}, \\
\varepsilon_{22}^{*} &= B_{22} + x_1^2 B_{2211} + x_2^2 B_{2222}, \\
\varepsilon_{12}^{*} &= x_1 x_2 B_{1212}.
\end{aligned} \tag{8}$$

Furthermore, by observing the symmetric and anti-symmetric property of the normal and shear components of the induced strain field and by invoking the material orthotropy and isotropy, one can deduct from Eq. (5) a following set of algebraic equations for the unknown coefficients, Bs:

$$\begin{aligned}
&\Delta C_{\alpha\alpha 11} L_{11}(\mathbf{0}) + \Delta C_{\alpha\alpha 22} L_{22}(\mathbf{0}) - C^{0}_{\alpha\alpha 11} B_{11} - C^{0}_{\alpha\alpha 22} B_{22} = -\Delta C_{\alpha\alpha 11}\varepsilon_{\infty 11} - \Delta C_{\alpha\alpha 22}\varepsilon_{\infty 22}, \\
&\frac{1}{2}\Delta C_{\alpha\alpha 11}\frac{\partial^2}{\partial x_1^2} L_{11}(\mathbf{0}) + \frac{1}{2}\Delta C_{\alpha\alpha 22}\frac{\partial^2}{\partial x_1^2} L_{22}(\mathbf{0}) - C^{0}_{\alpha\alpha 11} B_{1111} - C^{0}_{\alpha\alpha 22} B_{2211} = 0, \\
&\frac{1}{2}\Delta C_{\alpha\alpha 11}\frac{\partial^2}{\partial x_2^2} L_{11}(\mathbf{0}) + \frac{1}{2}\Delta C_{\alpha\alpha 22}\frac{\partial^2}{\partial x_2^2} L_{22}(\mathbf{0}) - C^{0}_{\alpha\alpha 11} B_{1122} - C^{0}_{\alpha\alpha 22} B_{2222} = 0, \\
&\Delta C_{1212}\frac{\partial^2}{\partial x_1 \partial x_2} L_{12}(\mathbf{0}) - C^{0}_{1212} B_{1212} = 0,
\end{aligned} \tag{9}$$

where

$$\begin{aligned}
L_{\alpha\beta}(\mathbf{x}) = {} & D_{\alpha\beta 11}(\mathbf{x})B_{11} + D_{\alpha\beta 22}(\mathbf{x})B_{22} + D_{\alpha\beta 1111}(\mathbf{x})B_{1111} + D_{\alpha\beta 1122}(\mathbf{x})B_{1122} + D_{\alpha\beta 2211}(\mathbf{x})B_{2211} \\
& + D_{\alpha\beta 2222}(\mathbf{x})B_{2222} + D_{\alpha\beta 1212}(\mathbf{x})B_{1212}, \quad (\alpha, \beta = 1, 2),
\end{aligned}$$

and the notation $L_{\alpha\beta}(\mathbf{0})$ and $(\partial^2/\partial x_1^2)L_{\alpha\beta}(\mathbf{0})$, etc., means that the L's and their second derivatives are evaluated at point (0,0), i.e., the origin of the coordinate system.

Once the coefficients Bs, thus ε_{ij}^{*}, are determined, the elastic fields in the inhomogeneity problem can be obtained from the corresponding results of the equivalent inclusion problem. It remains now to derive Eshelby tensor Ds mentioned above for a polygon-shaped inclusion with eigenstrains given in the form of polynomials of the coordinates and the complete elastic fields of the "equivalent" inclusion problem. That will be the subject of next Section 3.

3. An inclusion problem with polynomial eigenstrains

3.1. Formulation

Consider an infinite, elastic, homogeneous, and isotropic media having an inclusion Ω with an eigenstrain ε^*_{ij}. The eigenstrains are so defined that they assume some functional values in Ω but vanishes outside Ω. The induced strain ε_{ij} and the resulting stress σ_{ij} are given by (Mura, 1987)

$$\varepsilon_{ij}(\mathbf{x}) = \frac{1}{8\pi(1-\nu)}\left\{\Psi_{kl,klij} - 2\nu\Phi_{kk,ij} - 2(1-\nu)(\Phi_{ik,kj} + \Phi_{jk,ki})\right\}, \tag{10}$$

$$\sigma_{ij}(\mathbf{x}) = \begin{cases} C_{ijkl}(\varepsilon_{kl} - \varepsilon^*_{kl}), & \text{inside } \Omega, \\ C_{ijkl}\varepsilon_{kl}, & \text{outside } \Omega, \end{cases} \tag{11}$$

where

$$\begin{aligned} \Psi_{ij} &= \int_\Omega\int \varepsilon^*_{ij}\left|\mathbf{x}-\mathbf{x}'\right| \mathrm{d}\mathbf{x}', \\ \Phi_{ij} &= \int_\Omega\int \frac{\varepsilon^*_{ij}}{|\mathbf{x}-\mathbf{x}'|}\,\mathrm{d}\mathbf{x}', \end{aligned} \tag{12}$$

$\mathrm{d}\mathbf{x}' = \mathrm{d}x'_1 \cdot \mathrm{d}x'_2 \cdot \mathrm{d}x'_3$, while a prime indicates partial differentiation. The functions ψs and ϕs are known as the bi-harmonic and harmonic potentials, respectively. It should be noted that the induced strain field given by Eq. (10) is valid for both interior and exterior points of Ω.

Now, assume that the eigenstrains ε^*_{ij} are given in the form of Eq. (6). Substitution of Eq. (6) into Eq. (12) yields

$$\begin{aligned} \Psi_{ij} &= B_{ij}\psi + B_{ijk}\psi_k + B_{ijkl}\psi_{kl} + \cdots, \\ \Phi_{ij} &= B_{ij}\phi + B_{ijk}\phi_k + B_{ijkl}\phi_{kl} + \cdots, \\ \psi &= \int_\Omega\int \left|\mathbf{x}-\mathbf{x}'\right| \mathrm{d}\mathbf{x}', \\ \psi_{k\cdots l} &= \int_\Omega\int x_k \ldots x_l\left|\mathbf{x}-\mathbf{x}'\right| \mathrm{d}\mathbf{x}', \\ \phi &= \int_\Omega\int \frac{1}{|\mathbf{x}-\mathbf{x}'|}\,\mathrm{d}\mathbf{x}', \\ \phi_{k\cdots l} &= \int_\Omega\int \frac{x_k \cdots x_l}{|\mathbf{x}-\mathbf{x}'|}\,\mathrm{d}\mathbf{x}'. \end{aligned} \tag{13}$$

Substitution of Eq. (13) into Eq. (10) gives

$$\varepsilon_{ij}(\mathbf{x}) = D_{ijkl}(\mathbf{x})B_{kl} + D_{ijklm}(\mathbf{x})B_{klm} + D_{ijklmn}(\mathbf{x})B_{klmn} + \cdots, \tag{14}$$

where

$$8\pi(1-\nu)D_{ijklm\cdots n} = \psi_{m\ldots n,klij} - 2\nu\delta_{kl}\phi_{m\ldots n,ij} - (1-\nu)(\delta_{il}\phi_{m\ldots n,kj} + \delta_{jl}\phi_{m\ldots n,ki} + \delta_{ik}\phi_{m\ldots n,lj} + \delta_{jk}\phi_{m\ldots n,li}), \tag{15}$$

and δ_{kl} is the Kronecker delta.

From Eq. (14), it is clear that D_{ijkl}, D_{ijklm}, and D_{ijklmn} are the Eshelby tensors for an inclusion with eigenstrains given by constant, linear and quadratic functions of the coordinates, respectively. In order to determine these tensors, one need to evaluate ψ, $\psi_{m\ldots n}$, ϕ, $\phi_{m\ldots n}$ and their derivatives. Recently, Rodin (1996) has proposed a simple algorithm to compute these quantities. A brief description of that algorithm will be presented in Section 3.2.

So far, all formulas are given for a 3-D problem. In relevance to the present load attraction problem, these formulas must be specialized to a 2-D elasticity. Since most of these formulas are quite general, they also apply well to the 2-D case without any change, except for the expressions given in Eqs. (12) and (13). By considering the inclusion Ω as an infinite cylinder with a polygon-shaped cross-section, one can obtain formulas corresponding to Eqs. (12) and (13) for a plane strain case by integrating those equations in the third direction (Rodin, 1996; MacMillan, 1958). These new formulas will be given explicitly in Section 3.2.

3.2. Computational algorithm

As before, we restrict our presentation to the case of a polygon-shaped inclusion symmetric with respect to both coordinate axes and with eigenstrain given by Eq. (8). For simplicity, all formulation presented in this section has been derived for plane strain condition. The formulation can be easily modified for the plane stress case as in the present load attraction problem by replacing the Young modulus E with $E(1+2\nu)/(1+\nu)^2$ and the Poisson ratio ν with $\nu/(1+\nu)$, while keeping the shear modulus μ unchanged.

The Rodin's algorithm is implemented in three stages. First, the inclusion domain Ω is decomposed into a set of triangular elements (subregions) in such a way that **x**, the point where the solution is evaluated, is a common vertex of all the elements (Fig. 2). Second, ψ, $\psi_{m\ldots n}$, ϕ, $\phi_{m\ldots n}$ and their derivatives are calculated for each element in its *local* coordinate system. Third, tensors Ds are assembled from the elemental contributions after appropriate coordinate transformation from local to a common, global coordinate system.

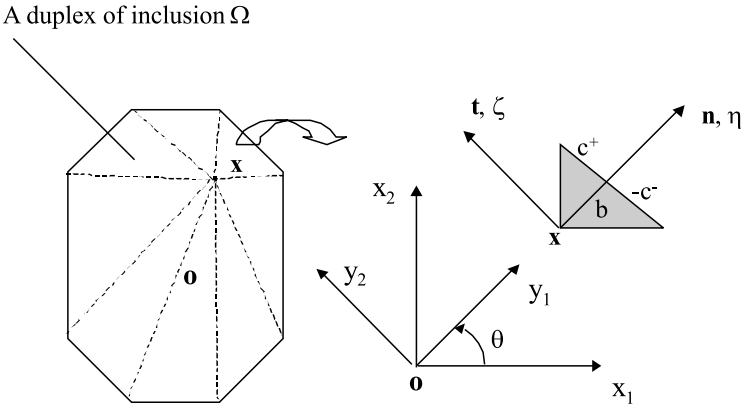

Fig. 2. Two dimensional construction of duplexes used in Rodin's algorithm. Global and two local coordinate systems for a typical duplex are also defined in the figure.

Using Rodin's (1996) terminology, the triangular elements made up of domain Ω are called duplexes and they are referred to as simplexes for the case of right triangles. Since a duplex can be formed from two simplexes and the computation for latter is more efficient than that for the former, we will derive the elemental Eshelby tensors for a simplex in the local coordinate system.

In Sections 1 and 2, we have referred to only one coordinate system, i.e., the global coordinate system **x** with an origin at the center of Ω as shown in Fig. 2. Referring to Fig. 2, let us define the element coordinate system mentioned in the above paragraph as follows. It has the origin at **x,** basis vectors (**n**,**t**), where **n** is a unit vector outward normal to the edge and **t** is the tangent vector, and the corresponding coordinates (η, ζ). In these coordinates, the positions of vertices are represented by the pairs (b, c^+) and (b, c^-). For a convex polygon, b is positive when **x** is an interior point of Ω and becomes negative otherwise.

It was shown (Rodin, 1996) that computations of the Eshelby tensors are simpler if they are carried out in this local coordinate system. In fact, all results given in the cited reference for a simplex with uniform eigenstrains are obtained in the local coordinate system. Since the present problem deals with polynomial eigenstrains, computations along these lines for a simplex requires introducing a second local coordinate system, i.e., **y**, which is parallel to the element coordinate system but with the origin at same point as that in the global coordinate system (Fig. 2). It should be reminded that the eigenstrains given in Eq. (8) are expressed in a form of polynomials of *global* coordinates. From the work of Rodin (1996), for a two-dimensional (plane strain) simplex with one of the vertices defined by (b, c), ψ, $\psi_{m\ldots n}$, ϕ, $\phi_{m\ldots n}$ in Eq. (13) can be rewritten as

$$
\begin{aligned}
\psi &= -\frac{1}{2}\int_0^b \mathrm{d}\eta \int_0^{c\eta/b} (\eta^2+\zeta^2)\ln(\eta^2+\zeta^2)\mathrm{d}\zeta,\\
\psi_{m\ldots n} &= -\frac{1}{2}\int_0^b \mathrm{d}\eta \int_0^{c\eta/b} (x_m\cdots x_n)\cdot(\eta^2+\zeta^2)\ln(\eta^2+\zeta^2)\mathrm{d}\zeta,\\
\phi &= -\int_0^b \mathrm{d}\eta \int_0^{c\eta/b} \ln(\eta^2+\zeta^2)\mathrm{d}\zeta,\\
\phi_{m\ldots n} &= -\int_0^b \mathrm{d}\eta \int_0^{c\eta/b} (x_m\cdots x_n)\ln(\eta^2+\zeta^2)\mathrm{d}\zeta,
\end{aligned}
\tag{16}
$$

where

$$
\begin{aligned}
x_1 &= (y_1+\eta)\cos\theta - (y_2+\zeta)\sin\theta,\\
x_2 &= (y_1+\eta)\sin\theta + (y_2+\zeta)\cos\theta,
\end{aligned}
\tag{17}
$$

and y_α and θ are independent of η, ζ. The logarithmic terms appear in Eq. (16) as a result of integration of Eq. (13) in the third direction as mentioned in the last paragraph of Section 3.1.

For the eigenstrains given by Eq. (8), one needs to evaluate four potential pairs (ϕ,ψ), (ϕ_{11},ψ_{11}), (ϕ_{22},ψ_{22}) and (ϕ_{12},ψ_{12}), which correspond to the eigenstrains B_{ij}, $x_1^2 B_{ij11}$, $x_2^2 B_{ij22}$ and $x_1x_2B_{ij12}$, respectively. However, since the Eshelby tensor for a constant eigenstrain B_{ij} has been already derived explicitly (Rodin, 1996), only the last three potential pairs are needed to be evaluated. It can be shown, after some lengthy algebra, that these potential pairs are given by

$$
\begin{aligned}
-\phi_{11}(\mathbf{y},b,c) &= \left(y_1^2\cos^2\theta + y_2^2\sin^2\theta - 2y_1y_2\cos\theta\sin\theta\right)I_0^0 + I_0^2\cos^2\theta + I_2^0\sin^2\theta + (2y_1\cos^2\theta \\
&\quad - 2y_2\cos\theta\sin\theta)I_0^1 + (2y_2\sin^2\theta - 2y_1\cos\theta\sin\theta)I_1^0 - 2\cos\theta\sin\theta I_1^1, \\
-2\psi_{11}(\mathbf{y},b,c) &= \left(y_1^2\cos^2\theta + y_2^2\sin^2\theta - 2y_1y_2\cos\theta\sin\theta\right)(I_0^2 + I_2^0) + (I_2^2 + I_0^4)\cos^2\theta + (I_4^0 + I_2^2)\sin^2\theta \\
&\quad + (2y_1\cos^2\theta - 2y_2\cos\theta\sin\theta)(I_2^1 + I_0^3) + (2y_2\sin^2\theta - 2y_1\cos\theta\sin\theta)(I_1^2 + I_3^0) \\
&\quad - 2\cos\theta\sin\theta(I_3^1 + I_1^3), \\
-\phi_{22}(\mathbf{y},b,c) &= \left(y_1^2\sin^2\theta + y_2^2\cos^2\theta + 2y_1y_2\cos\theta\sin\theta\right)I_0^0 + I_0^2\sin^2\theta + I_2^0\cos^2\theta + (2y_1\sin^2\theta \\
&\quad + 2y_2\cos\theta\sin\theta)I_0^1 + (2y_2\cos^2\theta + 2y_1\cos\theta\sin\theta)I_1^0 + 2\cos\theta\sin\theta I_1^1, \\
-2\psi_{22}(\mathbf{y},b,c) &= \left(y_1^2\sin^2\theta + y_2^2\cos^2\theta + 2y_1y_2\cos\theta\sin\theta\right)(I_0^2 + I_2^0) + (I_2^2 + I_0^4)\sin^2\theta + (I_4^0 + I_2^2)\cos^2\theta \\
&\quad + (2y_1\sin^2\theta + 2y_2\cos\theta\sin\theta)(I_2^1 + I_0^3) + (2y_2\cos^2\theta + 2y_1\cos\theta\sin\theta)(I_1^2 + I_3^0) \\
&\quad + 2\cos\theta\sin\theta(I_3^1 + I_1^3),
\end{aligned} \tag{18}
$$

$$
\begin{aligned}
-\phi_{12}(\mathbf{y},b,c) &= \left[y_1^2\cos\theta\sin\theta - y_2^2\cos\theta\sin\theta + y_1y_2(\cos^2\theta - \sin^2\theta)\right]I_0^0 + I_0^2\cos\theta\sin\theta - I_2^0\cos\theta\sin\theta \\
&\quad + \left[2y_1\cos\theta\sin\theta + y_2(\cos^2\theta - \sin^2\theta)\right]I_0^1 - \left[2y_2\cos\theta\sin\theta - y_1(\cos^2\theta - \sin^2\theta)\right]I_1^0 \\
&\quad + (\cos^2\theta - \sin^2\theta)I_1^1, \\
-\psi_{12}(\mathbf{y},b,c) &= \left[y_1^2\cos\theta\sin\theta - y_2^2\cos\theta\sin\theta + y_1y_2(\cos^2\theta - \sin^2\theta)\right]\left(I_0^2 + I_2^0\right) + \left(I_2^2 + I_0^4\right)\cos\theta\sin\theta \\
&\quad - (I_4^0 + I_2^2)\cos\theta\sin\theta + \left[2y_1\cos\theta\sin\theta + y_2(\cos^2\theta - \sin^2\theta)\right]\left(I_2^1 + I_0^3\right) - [2y_2\cos\theta\sin\theta \\
&\quad - y_1(\cos^2\theta - \sin^2\theta)\left]\left(I_1^2 + I_3^0\right) + (\cos^2\theta - \sin^2\theta)\left(I_3^1 + I_1^3\right),\right.
\end{aligned}
$$

where

$$
I_{\mathrm{p}}^q(b,c) = \int_0^b \int_0^{c\eta/b} \eta^q \zeta^{\mathrm{p}} \ln(\zeta^2 + \eta^2)\,\mathrm{d}\zeta\,\mathrm{d}\eta. \tag{19}
$$

The integral $I_{\mathrm{p}}^q(b,c)$ is straightforward to evaluate; however, its explicit form is omitted from here as it can be found in Gradshteyn and Ryzhik (1965).

To obtain the Eshelby tensors Ds in global coordinate system, the potentials must be differentiated with respect to $\mathbf{x}$ as prescribed in Eq. (15). However, as mentioned in the beginning of this section, it is more convenient to obtain these tensors in the local coordinate system $\mathbf{y}$. By denoting the Eshelby tensors Ds in the local coordinate system as $\overline{D}$s, $\overline{D}$s can be obtained in a straight forward manner from Eq. (15) by differentiating the potentials appropriately with respect to $\mathbf{y}$ while observing that (Rodin, 1996):

$$
\begin{aligned}
&b = b(\mathbf{x}), \\
&c = c(\mathbf{x}), \\
&\frac{\partial b}{\partial y_1} = \frac{\partial c}{\partial y_2} = -1, \\
&\frac{\partial b}{\partial y_2} = \frac{\partial c}{\partial y_1} = 0,
\end{aligned}
$$

and therefore,

$$\frac{\partial}{\partial y_1} f(\mathbf{y}, b, c) = \frac{\partial f}{\partial y_1} - \frac{\partial f}{\partial b},$$
$$\frac{\partial}{\partial y_2} f(\mathbf{y}, b, c) = \frac{\partial f}{\partial y_2} - \frac{\partial f}{\partial c}. \tag{20}$$

Even though the above task is straight forward, however, it involves extremely laborious calculation. One therefore should rely on symbolic computations to carry out that task. In fact, all explicit expressions for $\overline{D}$s in the present work have been derived with the aid of Mathematica (Wolfram, 1991). In contrast to the case of a constant eigenstrain, the expressions of $\overline{D}$s for quadratic eigenstrains are too lengthy to be included here due to space limitation.

So far we have outlined only the algorithm to compute Eshelby tensors $\overline{D}(\mathbf{y})$ and $D(\mathbf{x})$ but not the second derivative of $D(\mathbf{x})$s with respect to $\mathbf{x}$ as required in Eq. (9) in Section 2. Two different methods have been considered in the present work to evaluate the second derivatives of $D(\mathbf{x})$s. The first method involves numerical differentiation of $D(\mathbf{x})$s using central-difference scheme with error of order h^4 where h is the spacing between grid points (James et al., 1977). In this method, $D(\mathbf{x})$s must be computed at a number of points in a rectangular grid surrounding the point of interest. The second method is to use Mathematica (Wolfram, 1991) to derive $\partial\overline{D}/\partial\mathbf{y}$s and $\partial^2\overline{D}/\partial\mathbf{y}^2$s analytically and then to transform these derivatives into $\partial^2 D/\partial\mathbf{x}^2$s through appropriate coordinate transformation. It turns out that both methods yield almost identical results for all patch geometries considered. However, the implementation of the former method is much simpler.

Stresses near the vertex of Ω are of practical importance in design and analysis of bonded repairs and therefore needed to be addressed. As pointed out by Rodin (1996), the stress field near the vertex of Ω under constant eigenstrain takes the following asymptotic form:

$$\mathbf{s} \approx \frac{1}{8\pi(1-\nu)} (\mathbf{M}_1 - \mathbf{M}_2)\mathbf{B} \ln\left(\frac{\ell}{r}\right), \tag{21}$$

where

$$\mathbf{s} = \begin{Bmatrix} \sigma_{11} \\ \sigma_{22} \\ \sigma_{12} \end{Bmatrix}, \qquad \mathbf{B} = \begin{Bmatrix} B_{11} \\ B_{22} \\ B_{12} \end{Bmatrix}, \tag{22}$$

subscripts 1 and 2 denote the edges forming the vertex; ℓ is a representative edge length; r is the distance from the vertex; $\mathbf{M}_1$ and $\mathbf{M}_2$ are represented by the same matrix in the basis $(\mathbf{n}_1, \mathbf{t}_1)$ and $(\mathbf{n}_2, \mathbf{t}_2)$, respectively. That matrix is

$$\mathbf{M} = \frac{1}{2} \begin{bmatrix} 0 & 0 & -1+4\nu \\ 0 & 0 & -3+4\nu \\ -1 & -3 & 0 \end{bmatrix}. \tag{23}$$

It can be shown that the stress field near the vertices of Ω with eigenstrains prescribed by Eq. (8) also takes the same asymptotic form of Eq. (21), except that $\mathbf{B}$ is now defined as:

$$\mathbf{B} = \begin{Bmatrix} B_{11} + x_1^2 B_{1111} + x_2^2 B_{1122} \\ B_{22} + x_1^2 B_{2211} + x_2^2 B_{2222} \\ x_1 x_2 B_{1212} \end{Bmatrix}. \tag{24}$$

At this point, we are ready to devote our effort in solving the load attraction problem in bonded repairs.

4. Application to the load attraction problem of bonded repairs

Consider an infinite isotropic skin sheet reinforced with a polygon-shaped, bonded patch and the sheet is subjected to remote biaxial stresses similar to what is shown in Fig. 1. This problem can be analyzed by the equivalent inclusion method mentioned in Section 2 with the following simplifying assumptions:

- All material behavior is linearly elastic.
- All sheet and patch materials are in a state of generalized plane stress.
- The patch is modeled as an integral part of the skin using inclusion analogy.

Additional effects such as the effect of bending, thermal stresses associated with the curing processing and the variation of operating temperatures, and the effect of elastic–plastic adhesive can be superimposed on the results obtained from this basic model as they are more conveniently treated in a separate analysis (for example, Rose, 1988; Fredell, 1994). However, it is beyond the scope of this work to include those effects.

In Section 2, we consider a problem of an infinite isotropic sheet containing an inhomogeneity under remote biaxial stresses. In order to apply the results obtained from that section to the present load attraction problem, one needs to establish the material properties of the inhomogeneity which are equivalent to those of the patched skin. This had been done (Rose, 1988; Fredell, 1994) with key results summarized below for plane stress condition:

$$\begin{aligned} A_x^{\mathrm{I}} &= (A_x^0 t_0 + A_x^{\mathrm{p}} t_{\mathrm{p}})/t_{\mathrm{I}}, \\ A_y^{\mathrm{I}} &= (A_y^0 t_0 + A_y^{\mathrm{p}} t_{\mathrm{p}})/t_{\mathrm{I}}, \\ v_{xy}^{\mathrm{I}} &= (v_{xy}^0 A_y^0 t_0 + v_{xy}^{\mathrm{p}} A_y^{\mathrm{p}} t_{\mathrm{p}})/(A_y^0 t_0 + A_y^{\mathrm{p}} t_{\mathrm{p}}), \\ \mu^{\mathrm{I}} &= (\mu^0 t_0 + \mu^{\mathrm{p}} t_{\mathrm{p}})/t_{\mathrm{I}}, \end{aligned} \tag{25}$$

where A_x, A_y, v_{xy} and μ are the material constants which appear in the stress–strain relation for an orthotropic plate as follows

$$\begin{Bmatrix} \sigma_{11} \\ \sigma_{22} \\ \sigma_{12} \end{Bmatrix} = \begin{bmatrix} A_x & v_{xy}A_y & 0 \\ v_{xy}A_y & A_y & 0 \\ 0 & 0 & \mu \end{bmatrix} \begin{Bmatrix} \varepsilon_{11} \\ \varepsilon_{22} \\ \gamma_{12} \end{Bmatrix}, \tag{26}$$

$$A_x \equiv \frac{E_x}{1 - v_{xy}v_{yx}}, \qquad A_y \equiv \frac{E_y}{1 - v_{xy}v_{yx}},$$

t is thickness while the superscript or subscripts I, 0 and p signify the inhomogeneity, skin and patch, respectively. For an isotropic plate, $E_x = E_y = E$, $v_{xy} = v_{yx} = v$, and $\mu = E/2(1 + v)$. It should be noted that Eq. (25) has been derived from the following two conditions (Rose, 1981):

$$\begin{aligned} \sigma_{ij}^{\mathrm{I}} t_{\mathrm{I}} &= \sigma_{ij}^0 t_0 + \sigma_{ij}^{\mathrm{p}} t_{\mathrm{p}}, \\ \varepsilon_{ij}^{\mathrm{I}} &= \varepsilon_{ij}^0 = \varepsilon_{ij}^{\mathrm{p}}. \end{aligned} \tag{27}$$

The inhomogeneity thickness t_{I} can be chosen arbitrarily; however, t_{I} has been chosen to be the same as t_0 to enable a direct application of the solution established in Section 2. The stress field in the load attraction problem now can be determined by following the procedure outlined in Section 2, using constant or quadratic eigenstrain distribution approximation. The stress field in the patched region is calculated by first solving, for instance, Eq. (9) for the eigenstrains, then by computing the strains and stresses according to Eqs. (7) and (11), respectively, with the Eshelby tensors Ds being evaluated using the computational algorithm discussed in Section 3. The stresses in the skin and in the patch inside the reinforced area then can

be determined from the conditions prescribed in Eq. (27) once σ_{ij}^{I} has been calculated since $\varepsilon_{ij}^{0} = \varepsilon_{ij}^{\mathrm{p}} = \varepsilon_{ij}^{\mathrm{I}} = (C_{ijkl}^{\mathrm{I}})^{-1}\sigma_{kl}^{\mathrm{I}}$, $\sigma_{ij}^{0} = C_{ijkl}^{0}\varepsilon_{kl}^{0}$ and $\sigma_{ij}^{\mathrm{p}} = C_{ijkl}^{\mathrm{p}}\varepsilon_{kl}^{\mathrm{p}}$.

5. Numerical results

To assess the accuracy of the present analytical method, the stress field in a bonded patched sheet shown in Fig. 3, is obtained and compared with results from the finite element (FE) method. The length and width of the patch are six and four inches, respectively. The material properties and thickness of the skin and the patch as well as the far field stresses are given below:

Skin: isotropic

$$E = 10.3 \times 10^{6}\ \text{psi}, \quad \nu = 0.32, \quad t_0 = 0.063\ \text{inch}.$$

Patch: orthotropic

$$E_x = 2.7 \times 10^{6}\ \text{psi}, \quad E_y = 28 \times 10^{6}\ \text{psi}, \quad \nu_{xy} = 0.21, \quad G_{xy} = 0.8 \times 10^{6}\ \text{psi}, \quad t_{\mathrm{p}} = 0.025\ \text{inch},$$

$$\sigma_{\infty x} = 0, \quad \sigma_{\infty y} = 12500\ \text{psi}.$$

This problem has been solved approximately by the present analytical method when eigenstrains are assumed to be polynomials of degree zero (constant) and polynomials of degree two (quadratic) in the global position coordinates. The stresses along the line $y = 0$ are of special interest, as they are needed for stage II analysis of Rose's crack patching model. The normalized stress component σ_{yy} in the skin along the line $y = 0$ is plotted and compared with FE results in Fig. 4. FE results are obtained by using FRANC2D/L code (Swenson and James, 1997). All elements are 8-node isoparametric elements with the mesh being given in Fig. 5. In FE analysis, the adhesive is modeled as two-dimensional linear springs. Both typical and arbitrarily stiff adhesives are considered in the FE analysis. Typical values for shear modulus and thickness of an adhesive are 0.1×10^{6} psi and 0.005 inch, respectively. FE results for both cases of typical and stiff adhesives are presented in Fig. 4, along with the analytical predictions. A small oscillation in FE results

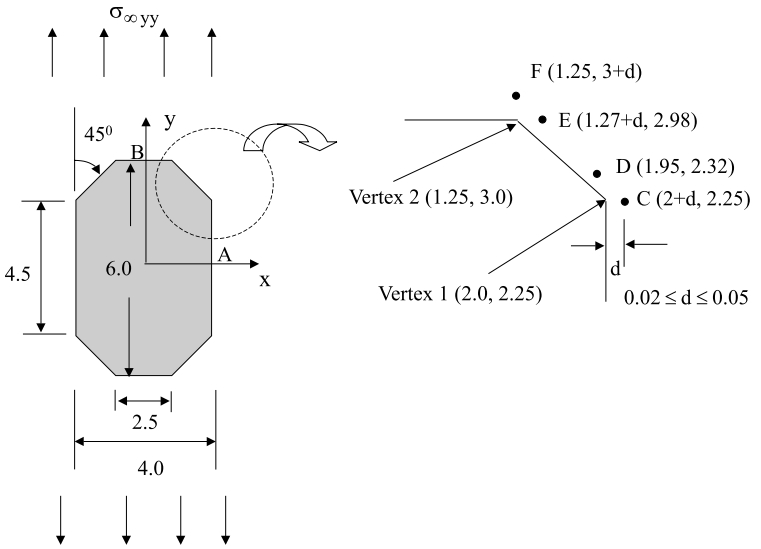

Fig. 3. Geometry of the example problem. The coordinates of the points where the stresses are evaluated and compared are also listed.

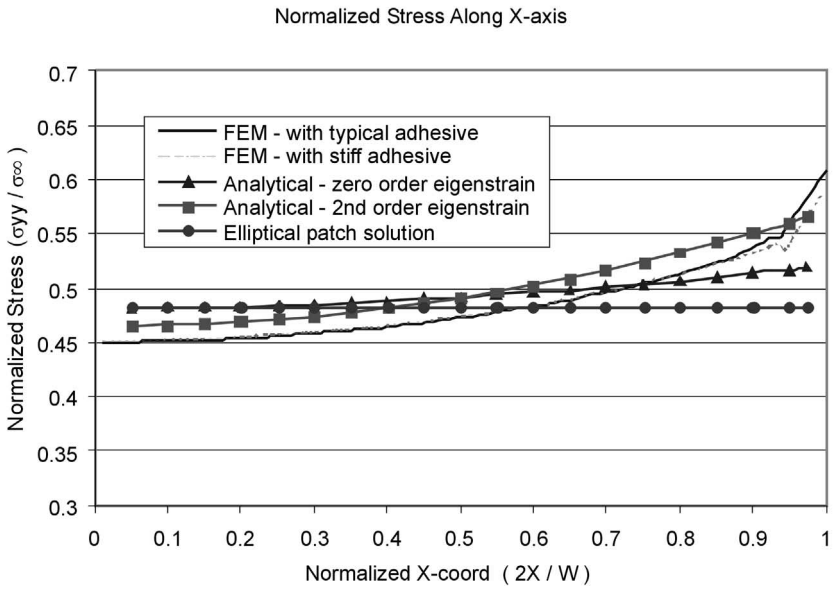

Fig. 4. Skin stress $\sigma_{yy}/\sigma_{\infty yy}$ underneath the patch and along the line $y = 0$.

near the edge of the patch is probably due to the discontinuity in skin stresses at the patch edge and also due to severe straining in the adhesive. From Fig. 4, analytical results are in excellent agreement with those from the finite element method. In general, analytical results based on the higher order eigenstrains are in better agreement with FE solutions. As the adhesive becomes stiffer, the difference in stresses between the analytical and FE methods becomes smaller, as expected. For reference, the normalized stress $\sigma_{yy}/\sigma_{\infty yy}$ in the patch near the centered region of Ω is also calculated and equals 2.3 and 2.1 according to constant and quadratic eigenstrain approximation, respectively, while the FE analysis using typical adhesive properties yields a result of 2.13.

The stresses in the skin just outside the patched area are also of practical interest due to possible high stress concentration or singularity there. These stresses are listed in Table 1 for various locations. The positions of these locations are defined in Fig. 3. It is well known that the stresses at the vertices are weakly singular and of the logarithmic nature. Stress comparisons between analytical and FE results at the vertices are thus difficult unless a very fine mesh is employed in those local regions. To avoid this difficulty and just for a qualitative comparison, stresses at small distance away from the vertices are reported in Table 1 (see Fig. 3 for positions of the reported points). The discrepancy between the analytical and FE method at points close to the vertices tends to be larger as their distance to the vertex decreases. It signifies the inability of the FE analysis in capturing the singularity with the presently employed mesh. For points adjacent to vertex 2, the agreement between two methods is fair for $d = 0.02$ (within 14%) and good for $d = 0.05$ (less than 10% difference). However, a much larger discrepancy is found for stresses at point C near vertex 1. It should be noted that the stress σ_{yy} is lower than the remote stress near vertex 1 but higher than the remote stress near vertex 2. The amplitudes of the logarithmic singularity at vertices 1 and 2 as obtained by the analytical method are in opposite sign as indicated in Table 2. The negative singularity near vertex 1 make the stress field there very complicated, resulting in a rapid stress oscillation in FE results (which have not been shown here). This may attribute in part to the observed large discrepancy. Nevertheless, since stresses at point C near vertex 1 are not critical from the design viewpoint, no further attempt is made to resolve this large discrepancy.

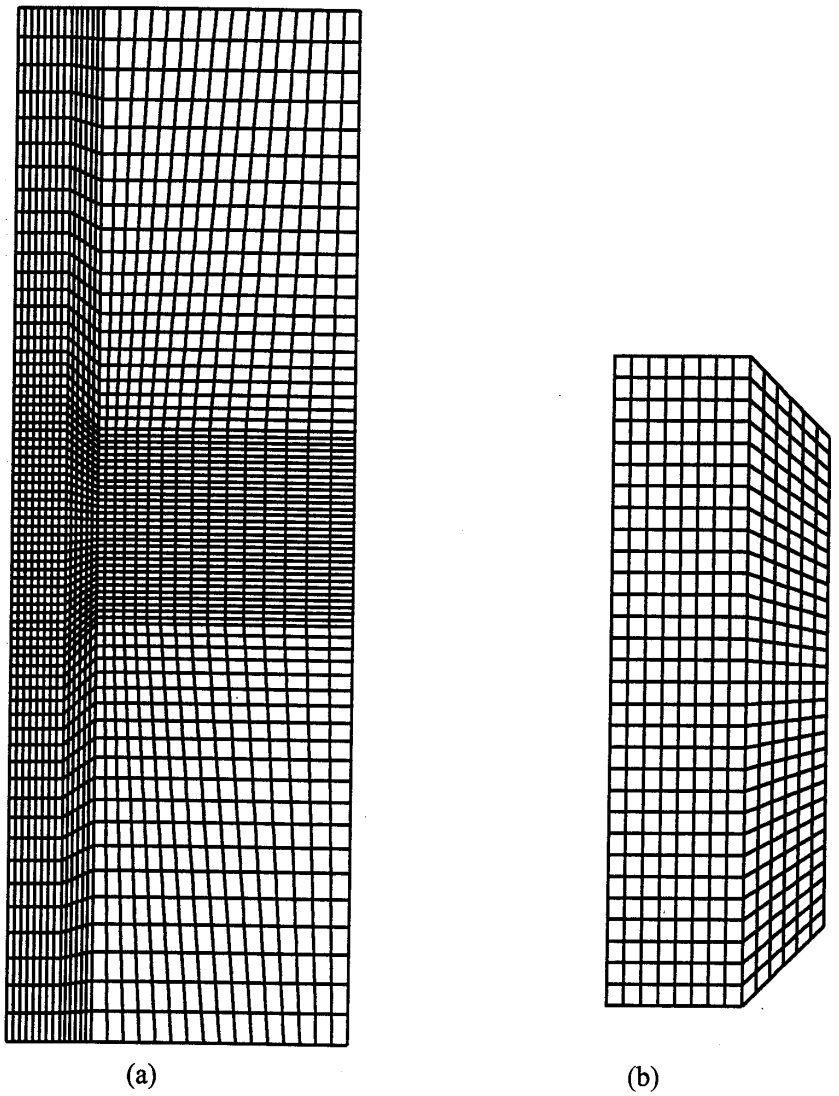

Fig. 5. Half FE model of the analyzing bonded problem. (a) Skin mesh and (b) patch mesh.

Table 1
A comparison of the skin stress $\sigma_{yy}/\sigma_{\infty yy}$ at various locations just outside the patched region by different methods[a]

Method	Point A	Point B	Point C	Point D	Point E	Point F
Analytical zeroth ordered	0.662	1.303	0.690 (0.629)	0.961	1.304 (1.346)	1.415 (1.479)
Analytical second ordered	0.644	1.278	0.680 (0.612)	0.998	1.330 (1.372)	1.435 (1.500)
FE based on stiff adhesive	0.620	1.240	0.804 (0.820)	0.922	1.278 (1.324)	1.376 (1.356)
FE based on typical adhesive	0.620	1.235	0.837 (0.850)	0.929	1.261 (1.288)	1.308 (1.322)

[a] The exact locations of these points are given in Fig. 3. For points C, E and F, the first number indicates the skin stress when $d = 0.05$, while the number given in the parenthesis is for $d = 0.02$.

Table 2
Amplitudes of the logarithmic singularity at vertices 1 and 2

Method	Amplitude M_{xx} in $\sigma_{xx} \approx M_{xx} \log r$		Amplitude M_{yy} in $\sigma_{yy} \approx M_{yy} \log r$	
	Vertex 1	Vertex 2	Vertex 1	Vertex 2
Analytical zeroth ordered	−123.2	123.2	−851.3	851.3
Analytical second ordered	−152.1	139.6	−980.6	851.3

Finally, since the solution for an elliptical patch is relatively simple to obtain and available (Rose, 1981), it is therefore of practical interest to compare the present results with those for an elliptical patch of the same aspect ratio A/B. This comparison would provide a basis for assessing whether or not elliptical patch solution provides a sufficiently accurate estimate of the effect of patch aspect ratio for design purposes. The stress in the skin underneath an elliptical patch with the same aspect ratio A/B is uniform and also plotted in Fig. 4 along with the FE and analytical results obtained previously for an octagonal patch. The elliptical patch solution is about 7% higher than FE result near center region. The normalized stresses in the skin at point A and B for the elliptical patch are found to be 0.55 and 1.39, respectively. The stress at point B in this case is approximately 12% higher than the corresponding FE result.

6. Conclusions

An analytical method for analyzing a bonded repair with a polygon-shaped patch is presented. The method is based on the equivalent inclusion method by Eshelby and employs Rodin's computational algorithm for a polygonal inclusion. The method is robust and versatile. In general, accurate results can be obtained from the present method without recourse to the FE method, where it requires a substantial effort of modeling or meshing. The present approach can also be applied to bonded sheets under thermal loads during bond formation or due to variation of operating temperatures. In fact, an extension of the present approach to address the residual thermal stress in a bonded sheet is in progress, and it will be discussed in a forthcoming paper.

References

Eshelby, J.D., 1957. The determination of the elastic field of an ellipsoidal inclusion and related problems. Proceedings of Royal Society (London) A 241, 376–396.

Fredell, R.S., 1994. Damage Tolerant Repair Techniques for Pressurized Aircraft Fuselages. Ph.D. Dissertation, Delft Technical University, The Netherlands.

Gradshteyn, L.S., Ryzhik, I.M., 1965. Table of Integrals, Series, and Products. Academic Press, New York.

James, M.L., Smith, G.M., Wolford, J.C., 1977. Applied Numerical Methods for Digital Computation with Fortran and CSMP. Harper & Row, New York.

Johnson, W.C., Earmme, Y.Y., Lee, J.K., 1980a. Approximation of the strain field associated with an inhomogeneous precipitate, part I: theory. Journal of Applied Mechanics 47, 775–780.

Johnson, W.C., Earmme, Y.Y., Lee, J.K., 1980b. Approximation of the strain field associated with an inhomogeneous precipitate, part II: The cuboidal inhomogeneity. Journal of Applied Mechanics 47, 781–788.

MacMillan, W.D., 1958. The Theory of the Potential. Dover, New York.

Moschovidis, Z.A., 1975. Two Ellipsoidal Inhomogeneities and Related Problems Treated by the Equivalent Inclusion Method. Ph.D. Dissertation, Northwestern University, Evanston.

Moschovidis, Z.A., Mura, T., 1975. Two ellipsoidal inhomogeneities by the equivalent inclusion method. Journal of Applied Mechanics 42, 847–851.

Mura, T., 1987. Micromechanics of Defects in Solids. Kluwer, Dordrecht, The Netherlands.

Nozaki, H., Taya, M., 1997. Elastic fields in a polygon-shaped inclusion with uniform eigenstrains. Journal of Applied Mechanics 64, 495–502.

Rose, L.R.F., 1981. An application of the inclusion analogy. International Journal of Solids and Structures 17, 827–838.

Rose, L.R.F., 1988. Theoretical analysis of crack patching. Bonded Repair of Aircraft Structures, in: Baker, A.A., Jones, R., (Eds.), Martinus Nijhoff, The Hague, pp. 77–105.

Rodin, G.J., 1996. Eshelby's inclusion problem for polygons and polyhedra. Journal of Mechanics and Physics of Solids 44, 1977–1995.

Sendeckyj, G.P., 1967. Ellipsoidal Inhomogeneity Problem. Ph.D. Dissertation, Northwestern University, Evanston.

Swenson, D., James, M., 1997. FRANC2D/L: A Crack Propagation Simulator for Plane Layered Structures, Version 1.4, User's Guide, Kansas State University.

Wolfram, S., 1991. Mathematica. Addison-Wesley, Reading, MA.